ACS APPLIED MATERIALS & INTERFACES

Research Article

www.acsami.org

Patterning of Nanodiamond Tracks and Nanocrystalline Diamond Films Using a Micropipette for Additive Direct-Write Processing

Alice C. Taylor, Robert Edgington, and Richard B. Jackman*

London Centre for Nanotechnology and Department of Electronic & Electrical Engineering, University College London, 17-19 Gordon Street, London WC1H 0AH, U.K.

ABSTRACT: The ability to pattern the seeding of nanodiamonds (NDs), and thus selectively control areas of diamond growth, is a useful capability for many applications, including photonics, microelectromechanical systems (MEMS) prototyping, and biomaterial design. A microprinting technique using a computer-driven micropipette has been developed to deposit patterns of ND monolayers from an unreactive water/glycerol ND ink to 5-μm resolution. The concentration and composition of the ND solution were optimized to realize high-density monolayers of NDs and consistent ND printing. Subsequent nanocrystalline diamond (NCD) patterns grown using chemical vapor deposition showed a high level of compliance with the printed ND pattern. This "direct-write", bottom-up, and additive process offers a versatile and simple alternative to pattern diamond. The process has the particular advantage that it does not require lithography or destructive processing such as reactive-ion etching (RIE) and, pertinently, does not involve reactive chemicals that could alter the surface chemistry of NDs. Furthermore, given that this process obviates the use of conventional lithography, substrates that are not suitable for lithographic processing (e.g., excessively small or three-dimensional structured substrates) can be inscribed with ND patterns. The technique also allows for the growth of discrete, localized, single-crystal nanodiamonds with applications in quantum technology.

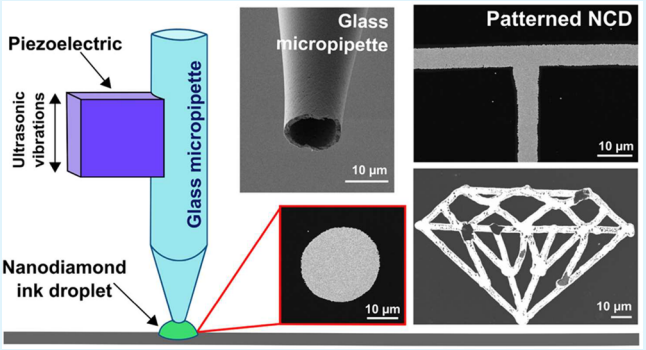

KEYWORDS: *diamond, nanodiamond, patterning, direct-write, microwave plasma-enhanced CVD*

INTRODUCTION

The exceptional properties of diamond make it a desirable material for the fabrication of microelectromechanical system (MEMS) devices[1,2] because of its attractive tribological[3] and mechanical properties, as well as high *Q*-factors being recorded on diamond microresonators.[4] However, the chemical[5] and electrochemical[6] inertness and the extreme mechanical stability[7] of diamond make it a difficult material to process. Nanocrystalline diamond (NCD) films produced by chemical vapor deposition (CVD) exhibit the excellent properties of naturally occurring diamond[8,9] while offering the prospect for the selective growth of diamond in specific locations, avoiding the need for three-dimensional pattern generation in thin-film diamond layers. Patterned diamond at the micrometer scale would offer desirable properties for many applications: Diamond bio-MEMS are highly desirably because of their biocompatibility[10] and diamond's strong resistance to bacterial colonization.[11] Other examples include diamond used for radio-frequency (RF) resonators;[12] scanning probe microscopy (SPM) probes as an all-diamond cantilever;[13] and diamond electrodes for sensor applications,[14] for patterning cells,[15−17] and for the fabrication of diamond microelectrode arrays (MEAs).[18−20]

Currently there are several methods to pattern NCD films: top-down reactive-ion etching (RIE),[18,21−27] laser ablation,[17,28,29] photolithographic etching,[30] and bottom-up selective nanodiamond (ND) particle seeding, all of which have their own merits. RIE is a destructive process in which photolithographic methods are used in conjunction with typically oxygen/argon RF plasmas to remove unwanted areas of NCD film. RIE patterning is advantageous in that it fits into conventional complementary metal−oxide−semiconductor (CMOS) processing work flows and can achieve submicrometer resolutions; however, difficulties are encountered when etching diamond because of the large resilience of diamond causing low etch selectivities for available hard masks, meaning that only shallow diamond films can be easily patterned using such an approach. Furthermore, O_2/Ar RF plasmas can be damaging to the underlying substrate materials upon which NCD films are deposited. More recently, selective seeding has emerged as a solution to counter the low selectivity of diamond RIE processing to allow the bottom-up patterning of ND and NCD films. Various methodologies have been employed to pattern ND seeds, including inkjet printing of diamond inks,[31,32] microcontact printing,[33] and ND seeding by electrostatic self-assembly.[34] Although these methods avoid the

Received: November 13, 2014
Accepted: February 11, 2015
Published: February 11, 2015

DOI: 10.1021/am507900a
ACS Appl. Mater. Interfaces 2015, 7, 6490−6495

problems associated with mask selectivity in diamond etching, photolithography is still required, and residual NDs can remain in nominally void pattern areas, leading to diamond growth in unwanted regions. To avoid this issue, Hébert et al. developed a method to combine the two processes by seeding with NDs, "fixing" NDs with a short CVD plasma exposure, removing ND seeds from void pattern areas with RIE, and subsequently growing patterned NDs into NCD films.[35]

Although all of these techniques have their merits, these processes still require photolithographic steps and the application of corrosive or reactive chemicals during processing, which could affect the surface chemistry of the deposited NDs. Here, a novel direct-write selective seeding method is described in which no photolithographic steps or corrosive chemicals are required. ND patterns are deposited using a micropipette, which can print a variety of solutions onto desired substrates in picoliter volumes through ultrasonic ejection of liquid. "Ink" constitution and printing parameters have been optimized, and the effects of varying the micropipette diameter were investigated. Postprinting, water and glycerol from the ink are evaporated at low pressures and temperatures to produce ND coatings of near-monolayer thickness in any desired pattern. Subsequent CVD growth leads to patterned NCD layers. This direct-write additive method allows for facile microfabrication of nanodiamond patterns on a variety of substrates and topographies, unlike photolithographic techniques, which are limited to planar surfaces and require corrosive chemicals. Finally, this method involves minimal wastage of NDs and can efficiently coat substrates using very small ND amounts, which is very important for applications in which sample amounts are scarce, such as the positioning of NDs with color centers (e.g., nitrogen−vacancy centers) on substrates.

EXPERIMENTAL METHODS

Selective Printing. A GIX II Microplotter (purchased from www.sonoplot.com (accessed January 2015)) was used in ambient conditions for the selective seeding of ND inks. The microplotter is a computer-controlled micropipette fluid dispensing system for the deposition of picoliter volumes of liquid to 5-μm precision. Liquids are drawn into the pipette from an ink well by capillary action and ejected by application of ultrasound to the pipette when in meniscal contact with a surface. The ultrasonic intensity is sufficiently low to avoid a spray ejection of liquid. The software program SonoDraw was used to design the desired patterns in which the ink would be printed on the surface. An applied piezo voltage of 20 V was used for every print as this was found to produce the most reliable and consistent printing. Printing speeds were varied from 100 to 10000 μm s^{-1} depending on the substrate and tip, typically being 2000 μm s^{-1} for silicon and 1000 μm s^{-1} for glass. Glass micropipettes were produced using a p-97 flaming/brown horizontal micropipette puller. Pulling parameters were optimized to produce a range of tips with inner diameters ranging between 1 and 30 μm.

Chemicals. Monodisperse detonation nanodiamonds (DNDs) (6−10 nm) were used throughout (New Metals & Chemicals Corporation, Tokyo, Japan). Various inks containing DNDs and glycerol (99.0% Sigma-Aldrich, 92.09 g mol^{-1}, 1414 cP) were produced and subjected to ultrahigh-power sonication using a VCX500 Vibra-cell sonicator with a cup horn accessory (100% amplitude, 3:2 duty cycle, water-cooled and temperature-controlled at <28 °C, 5 h) to fully disperse the DNDs and to ensure thorough glycerol/deionized (DI) water mixing.

Substrate Cleaning. Substrates were degreased in acetone, isopropyl alcohol (IPA), and then DI water (each for 5 min of sonication) to remove residues and dirt. Dust-free surfaces allow for higher-resolution printing, with reduced flow-back and also reduced contamination of particulates in the clean ND ink. With contamination, the NCD film quality suffers, as these particles act as renucleation sites, so the film contains more grain boundaries. Consequently, all substrates were thoroughly cleaned before use.

Ink Evaporation. A vacuum chamber (10^{-3} mbar, 50 °C, 5 min) was used to evaporate the glycerol/deionized water ink and leave the printed NDs in the desired pattern on the surface of the substrate. Vacuum evaporation was used to allow glycerol evaporation at low temperatures so as to not oxidize the NDs through heating (oxidation onset of ∼250 °C). The boiling point of glycerol at 10^{-3} mbar is 40 °C, so a temperature of 50 °C was used to ensure that all glycerol had evaporated. To obtain a regular seeding of NDs on the surface, it is important that a rapid evaporation of the ink is achieved. This helps to minimize the "coffee-ring" effect, whereby the ink dries toward the edge of the print, leaving a higher concentration of NDs around the ring.

Atomic Force Microscopy. Atomic force microscopy (AFM) measurements were carried out using a Veeco Dimension V instrument with aluminum coated silicon AFM probes (resonant frequency 190 kHz). The system was operated in tapping mode with a VT-103-3K acoustic/vibration isolation system and a VT-102 vibration isolation table at room temperature in air. AFM analysis was performed on ND patterns with varying ND concentrations, postevaporation, with a scan size of 2 μm. AFM Images were postprocessed with a median filter (3 × 3 kernel) using MATLAB 2012a software to remove noise and measurement artifacts. Surface coverage of NDs as a percentage was calculated using the threshold feature in ImageJ software.

Patterned Nanocrystalline Diamond Growth. Nanodiamond micropatterns were printed on degreased Si (native oxide), SiO_2 [plasma-enhanced (PE) CVD], and quartz wafers (5 min in acetone, 5 min in isopropanol alcohol, and 5 min in deionized water with low-power ultrasonication and N_2-gun drying). Print patterns were drawn using SonoDraw 1.1.3 software. Following ink evaporation, microwave-plasma-enhanced CVD (MPECVD) was performed using a SEKI model AX5010 PECVD reactor. The parameters for growth were 1500 W, 200 sccm H_2, and 1.4 sccm CH_4 (0.7%), with 30-min and 4-h growth times and a 5-min 5% CH_4 initial incubation period.

Scanning Electron Microscopy. Both the glass micropipettes and the NCD patterns were characterized using a Carl Zeiss XB1540 focused-ion-beam microscope with an accelerating voltage of 5 kV.

RESULTS AND DISCUSSION

Optimizing Ink Deposition. To achieve consistent and contiguous liquid deposition from a microplotter, optimization of the ink viscosity is essential. Various inks were prepared containing varying ratios of glycerol and deionized (DI) water, and dynamic viscosities were calculated using the parametrization reported by Cheng.[36] The viscosity of glycerol at 20 °C is much greater than that of water (1414 vs 1.75 cP). The optimum viscosity for printing was found for a mixture of 50 wt % glycerol and 50 vol % deionized water (4.83 cP), as illustrated in Figure 1a, with the values for the dynamic velocity of the ink plotted in Figure 1b. This ink had a low enough viscosity to allow effective flows from the tip, but a high enough viscosity to prevent reflow and clumping of the ink at pattern vertices.

In addition to improving print quality, glycerol reduces the evaporation rate of water as a result of the increase in intermolecular forces, which avoids the premature evaporation of ink and the uneven deposition of NDs biased toward the edges of features where evaporation concludes (i.e., the "coffee-ring" effect). Although glycerol reduces premature evaporation of the ink, the boiling point of glycerol at room pressure is 290 °C. Such temperatures could cause substrate damage, and there have been reports of ND oxidation occurring at temperatures as low as 300 °C,[37] which might lead to surface modification. Hence, a custom vacuum chamber was built to enable the use

DOI: 10.1021/am507900a
ACS Appl. Mater. Interfaces 2015, 7, 6490−6495

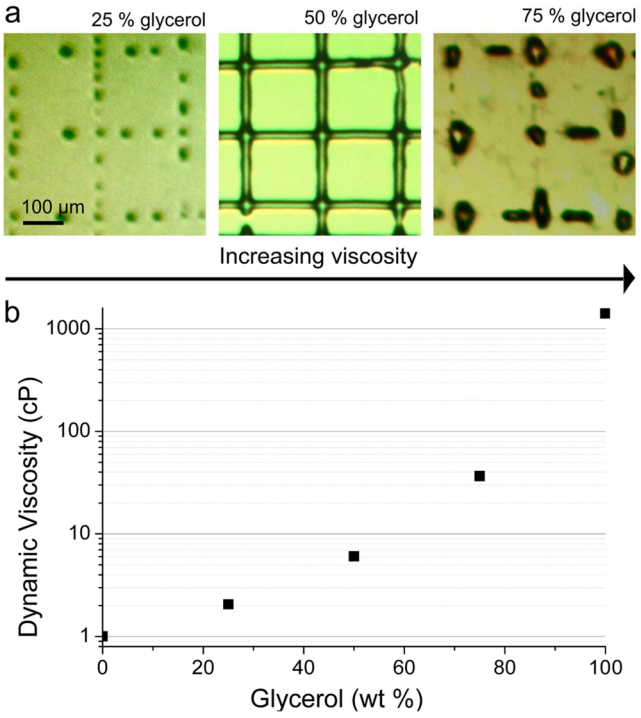

Figure 1. (a) Optical microscope images of grids printed using ND-containing inks on a glass substrate. The three images differ in glycerol percentage, which increases from left to right. Optimum printing is observed using an ink containing 50 wt % glycerol. (b) Solution viscosity as a function of weight percentage of glycerol. Optimum viscosity was found to be 6.04 cP.

of a lower vapor pressure of glycerol. A pressure of below 10^{-3} mbar was used to allow the evaporation of glycerol at 50 °C, which is sufficiently low to avoid chemical modification of the NDs.

ND Concentration. Having established an optimum ink viscosity, the effect of changing the ND concentration was investigated. To grow high-quality NCD patterns, it is important that the ND assembly on the surface coverage be as confluent and as close to monolayer as possible, as small particles (rather than aggregates) result in better film uniformity.[38] Therefore, it was important to determine the ND concentration that produced confluent ND seeding and near-monolayer coverage, so as to optimize subsequent NCD film growth and minimize ND usage. The effect of ND concentration on seeding was investigated using AFM.

Figure 2a shows AFM images of NDs seeded on silicon using a 30-μm tip and dot printing, with inks containing concentrations of NDs ranging from 0.025 to 0.15 g L^{-1}, following glycerol/DI water evaporation. The corresponding graph in Figure 2b shows the percentage coverage of the surface as a function of ND concentration. It can be seen that, for concentrations of 0.1 g L^{-1} and above, the coverage was 100%. For concentrations of less than 0.1 g L^{-1}, the coverage was incomplete; for example, at 0.75 g L^{-1}, the coverage was 82%. The monolayer-type coverage observed shows evidence of the occasional small aggregate being present in the printed region. This is better than other reported attempts at printing ND patterns. For example, Zhuang et al. used a microcontact printing technique for producing ND patterns, and the method was reported to be able to transfer only ND agglomerates and not individual ND particles.[33] As NCD quality is dependent on the size of the seed material and its uniformity, the method described here offers the prospect of better, denser NCD films.

Patterning. Figure 3 shows SEM images of CVD-grown patterned NCD films on silicon substrates with the ND seeds printed from a 0.1 g L^{-1} ND 50 wt % glycerol/DI water ink. The ND patterns were grown for between 30 min and 4 h (see figure captions for durations) using previously stated conditions. Figure 3a shows an array of lines printed using a tip with an inner diameter (i.d.) of 5 μm; the lines are spaced be 200 μm, and their width is approximately 7 μm. Consistent and clean printed lines are observed with a high level of pattern compliance and no residual NDs in void pattern regions. Figure 3b,c shows lines printed on Si using a 5-μm-i.d. tip. It can be seen that the edges (Figure 3d) of the lines are clean and that no additional processes are needed for the removal of unwanted NCD. Figure 3e displays the edge of a printed grid showing two intersecting lines, for a 5-μm-i.d. tip size. Figure 3f shows an NCD film printed with a void square in the middle; sharp lines and corners are observed, highlighting the high resolution of the printing method. Figure 3g shows the thinnest line achieved using this printing method: The line width is

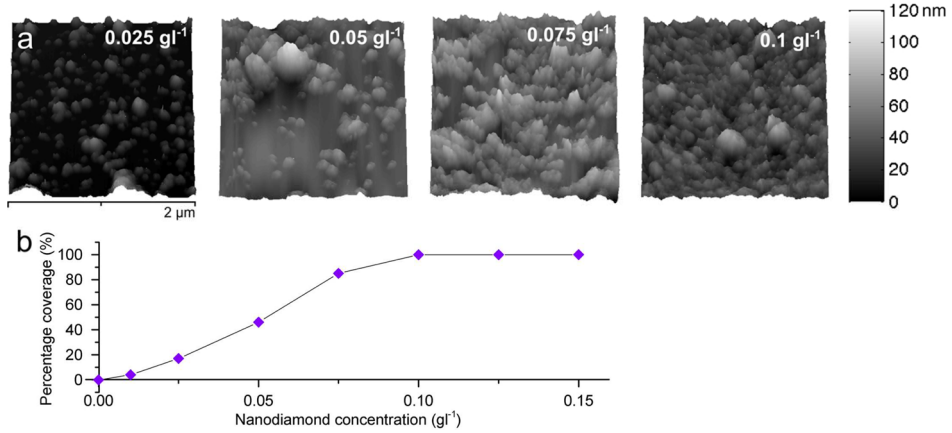

Figure 2. (a) AFM images (2 μm × 2 μm) of NDs seeded on silicon. Each image is of NDs after evaporation of a glycerol/deionized water ink. The resultant NDs are left seeded on the surface at varying coverage depending on the concentration of NDs in the ink. Concentrations shown are 0.025, 0.05, 0.075, and 0.1 g L^{-1}. Scans are representative of the whole patterned area and were selected at random over each print. (b) Corresponding percentage coverage of NDs on Si as a function of the concentration of NDs in the ink.

DOI: 10.1021/am507900a
ACS Appl. Mater. Interfaces 2015, 7, 6490−6495

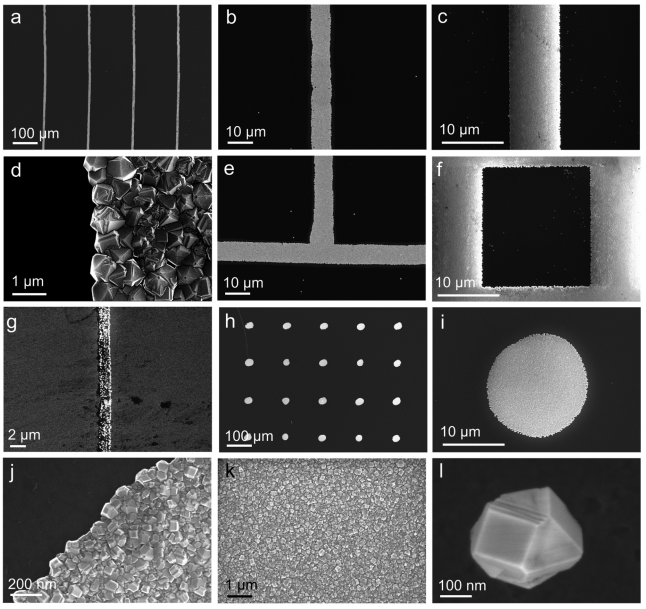

Figure 3. SEM images of patterned NCD films grown on silicon substrates using printed NDs as the seeds and MPECVD for the growth method. All inks consisted of 50 wt % glycerol and NDs at a concentration of 0.1 g L^{-1}; growth times varied from 30 min to 4 h; and other parameters for growth were 1500 W, 50 Torr, and 0.7% CH_4. (a–c) Series of lines printed using a 5-μm-i.d. tip, with a line width of approximately 7 μm after growth for 30 min. (d) Edge of the printed line shown in panel c. (e) Edge of a printed grid showing two intersecting lines, for 5-μm-i.d. tip size and growth for 30 min. (f) NCD outline of square grown for 4 h. (g) Line printed using q 1.5-μm-i.d. pipette, with a line width of ~2 μm after growth for 30 min. (h) Array of dots printed using a 15-μm-i.d. tip, grown for 1 h. (i) Individual printed NCD dot from panel h. (j) Edge of the printed dot shown in panel i. (k) Zoomed-in SEM image of the surface of a printed NCD region after 30 min of growth. (l) ND seed grown into an individual NCD grain for 4 h.

approximately 2 μm and was printed using a tip with an inner diameter of 1.5 μm. Figure 3h shows a 100-μm spaced array of printed NCD dots. Figure 3i shows one printed dot, with a diameter of approximately 20 μm, that was achieved using a tip with an inner diameter of 15 μm. Figure 3j shows the edge of the printed dot shown in Figure 3i; clean printed edges can be observed. The resolution of printing is limited by the mechanical movement of the machine, which has a 5-μm positioning resolution, and also by the size of the inner diamter of the pipette and ultrasonic power of the piezoelectric. Printed line artifacts are due to the slightly uneven motion of the tip during printing but can be minimized by securing the substrate during printing and altering the speed of the print accordingly. SonoDraw 1.1.3 software allows for the patterning of lines, dots, arcs, and filled regions, so any desired shape can be printed using this method. Figure 3k shows an SEM image of a high-quality NCD film, verified by the faceted texture of the NCD film, as well as the confluent, pinhole-free nature of the film, all of which can be ascribed to high-density, homogeneous seeding. The grain shown in Figure 3l was grown from a printed region where the ND concentration in the ink was 0.001 g L^{-1}. This resulted in an individual ND being grown into a small (~500-nm) single-crystal diamond. This capability is also of considerable interest because individually placed fluorescent NDs are key to several quantum information processing applications that are currently under investigation.

Tip Diameter versus Dot Diameter. To investigate the effect of inner diameter on dot deposition, a set of tips with varying diameters were prepared for printing. Different-sized tips were pulled using a horizontal micropipette puller, whereby controlling the speed of the tip pull changed the inner diameter. The inner diameters of the tips ranged from 1 to 30 μm. Figure 4a–d shows different tips of graded diameters alongside SEM images of their corresponding NCD dots on Si surfaces. All ND dots were subjected to 30-min growth using normal NCD conditions as previously stated. The minimum size of micropipette that can successfully print was found to be 1.5 μm. When attempting to print smaller than this, ink did not

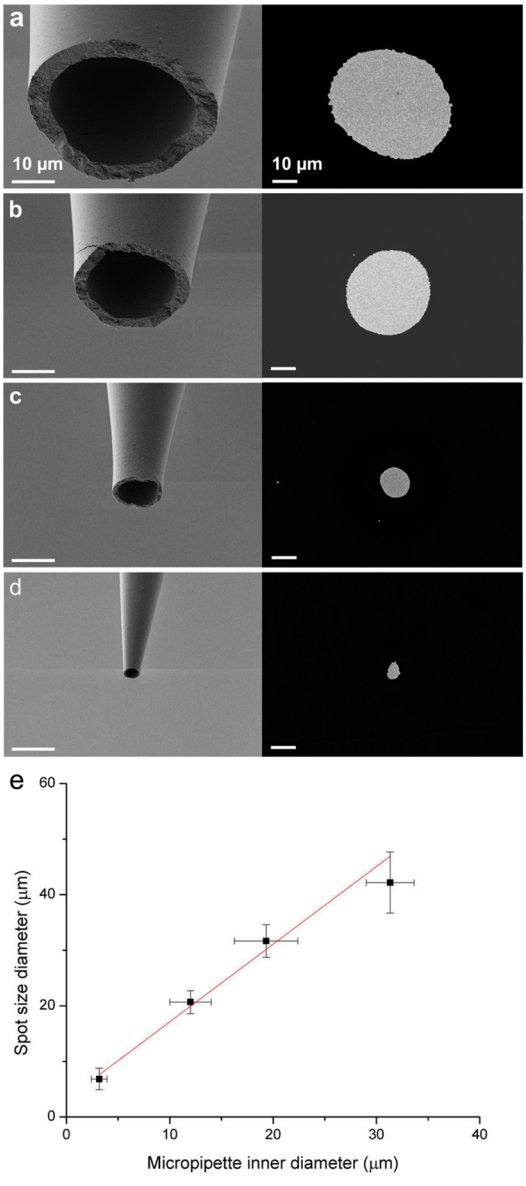

Figure 4. (a–d) SEM images of horizontally pulled glass micropipettes (left-hand column) and corresponding printed ND dots grown into NCD (right-hand column). The velocity of the pull was altered to produce micropipettes with the desired inner diameter. The velocity is in arbitrary units but ranged from (a) 8 to (d) 14 au, producing tips with inner diameters ranging from around 40 to 5 μm, respectively. (A tip with an inner diameter of 1.5 μm was pulled, but the SEM image is not available). (e) Corresponding graph showing how the micropipette inner diameter affects the diameter of the NCD dot.

DOI: 10.1021/am507900a
ACS Appl. Mater. Interfaces 2015, 7, 6490–6495

enter the micropipette due to capillary action failing to load the pipette. Figure 4e shows the relationship between tip inner diameter and NCD dot diameter (DD). The relationship is approximately linear, where the printed dot is slightly larger than the tip inner diameter (DD ≈ 3.15 + 1.40i.d.). For a 30-μm tip, the dot is roughly 45 μm, so an ink spreading of ca. 40% is observed. Micropipettes with an inner diameter of 30 μm were found to produce the most consistent printing.

NCD quality was investigated by SEM and Raman spectroscopy. One of the most important factors in determining the quality of thin-film diamond is surface roughness. The seeding quality and density of the nanodiamonds is paramount to this.[39] Various scratching and seeding techniques have been used to enhance ND nucleation density on foreign substrates. Scratching often results in a high nucleation density because the large diamond particles are imperfect and thus chip along grain boundaries, leaving smaller diamond particles on the surface that act as nucleation sites.[40] To obtain near-monolayer ND patterns, it is important to sonicate the ink immediately before printing. This ensures that the NDs are fully dispersed in solution and that as few as possible aggregates are present. The best results were achieved when ND inks were sonicated for at least 8 h immediately before printing. Nicely faceted NCD (4-h growth) can be seen in the SEM image in Figure 3e, confirming the quality of the ND seeding.

Figure 5 shows Raman spectra of the grown NCD dots. The diamond peak is observed at 1333 cm^{-1} for the 30-min growth

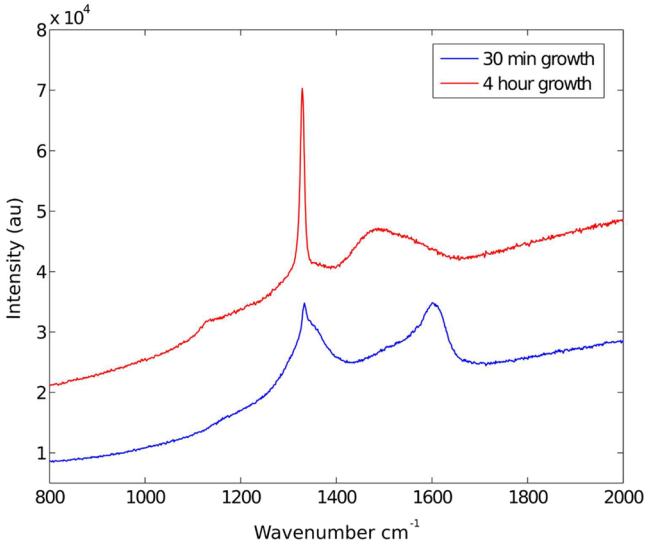

Figure 5. Raman spectra of NCD dots grown for 30 min and 4 h. Both spectra show the zero-phonon line present in diamond thin films.

and at 1329 cm^{-1} for the 4-h growth. This peak corresponds to the zero-phonon line of diamond, indicative of a high content of sp^3-bonded carbon. Peak broadening can be observed in the sp^3 peak for the 30-min growth because of the low crystallite size of diamond grains and the thinness of the film.[41] The red shift of the peak arises in phonon confinement in the NCD and is linear with grain size.[42] The narrowing of this peak for 4-h growth suggests that the film grain size is approaching the microscale. The broad peak observed at 1560 cm^{-1} in the 30-min-growth spectrum shows evidence of the nondiamond G-band, which arises from sp^2-carbon in-plane stretching mode, which can be assumed to be at the grain boundaries.[43]

CONCLUSIONS

An additive, lithography-free, inert bottom-up technique for producing nanodiamond tracks and nanocrystalline diamond patterns with a high pattern compliance has been established, with a lateral resolution of 5 μm and feature widths of ca. 2 μm. Patterning is achieved without the use of reactive chemicals, allowing for the preservation of ND surface chemistry. The patterning procedure was developed using an ultrasound driven plotter to deposit nanodiamond in glycerol/DI water inks. Printing was optimized by tailoring ink constitution, hardware parameters, and micropipette tip diameter to produce ND patterns with near-monolayer coatings with few agglomerates present. The effect of varying ND concentration on ND seeding was studied, and the relationship between tip diameter and dot size identified. Furthermore, low-density ND patterning was demonstrated, which makes this process a valuable method for studying the individual properties of NDs on substrates, for example, for quantum information processing applications. Postprinting, ink solvents were evaporated off using low-temperature vacuum evaporation to leave NDs in the desired pattern. The resultant ND patterns were used as the nucleation sites for NCD growth, and suspending the NDs in glycerol had no observable effects on the quality of the diamond film. Pertinently, this patterning technique allows for the selective seeding of NDs on a variety of substrates, including three-dimensional substrates that are not compatible with conventional lithography techniques, and with a high degree of control over the nature of the ND monolayers deposited. This method for diamond patterning provides a material type that has many potential applications, which range from use as a photonic crystal,[44] to use in bioelectronics[45] and MEMS applications including piezoelectric microresonators.[46]

AUTHOR INFORMATION

Corresponding Author

*E-mail: r.jackman@ucl.ac.uk.

Notes

The authors declare no competing financial interest.

ACKNOWLEDGMENTS

This work was performed as part of EU F7 Project "NEUROCARE" (no. 280433-2) and was partially supported by the U.K. Engineering and Physical Sciences Research Council (EPSRC, EP/F026110/1).

REFERENCES

(1) Luo, J. K.; Fu, Y. Q.; Le, H. R.; Williams, J. A.; Spearing, S. M.; Milne, W. I. Diamond and Diamond-like Carbon MEMS. *J. Micromech. Microeng.* **2007**, *17*, S147−S163.

(2) Bongrain, A.; Scorsone, E.; Rousseau, L.; Lissorgues, G.; Gesset, C.; Saada, S.; Bergonzo, P. Selective Nucleation in Silicon Moulds for Siamond MEMS Fabrication. *J. Micromech. Microeng.* **2009**, *19*, 074015.

(3) Williams, J. A.; Le, H. R. Tribology and MEMS. *J. Phys. D: Appl. Phys.* **2006**, *39*, R201−R214.

(4) Lu, J.; Cao, Z.; Aslam, D.; Sepúlveda, N.; Sullivan, J. Diamond Micro and Nano Resonators Using Laser Capacitive or Piezoresistive Detection. *IEEE Int. Conf. Nano/Micro Eng. Mol. Syst., 3rd* **2008**, 873−876.

(5) Krueger, A. Beyond the Shine: Recent Progress in Applications of Nanodiamond. *Lab Chip* **2011**, *21*, 12571.

(6) Fries, M. D.; Vohra, Y. K. Properties of Nanocrystalline Diamond Thin Films Grown by MPCVD for Biomedical Implant Purposes. *Diamond Relat. Mater.* **2004**, *13*, 1740−1743.

DOI: 10.1021/am507900a
ACS Appl. Mater. Interfaces 2015, 7, 6490−6495

(7) May, P. W. Diamond Thin Films: A 21st-Century Material. *Philos. Trans. R. Soc. A* **2000**, *358*, 473−495.
(8) Williams, O. A.; Nesladek, M. Growth and Properties of Nanocrystalline Diamond Films. *Phys. Status Solidi A* **2006**, *203* (13), 3375−3386.
(9) Philip, J.; Hess, P.; Feygelson, T.; Butler, J. E. Elastic, Mechanical, and Thermal Properties of Nanocrystalline Diamond Films. *J. Appl. Phys.* **2003**, *93*, 2164−2171.
(10) Tang, L.; Tsai, C.; Gerberich, W. W.; Kruckeberg, L.; Kania, D. R. Biocompatibility of Chemical-Vapour-Deposited Diamond. *J. Neurosci. Methods* **1995**, *16*, 483−488.
(11) Jakubowski, W.; Bartosz, G.; Niedzielski, P. Nanocrystalline Diamond Surface Is Resistant to Bacterial Colonization. *Diamond Relat. Mater.* **2004**, *13*, 1761−1763.
(12) Mortet, V.; Williams, O. A.; Haenen, K. Diamond: A Material for Acoustic Devices. *Phys. Status Solidi A* **2008**, *205*, 1009−1020.
(13) Malavé, A.; Oesterschulze, E. All-Diamond Cantilever Probes for Scanning Probe Microscopy Applications Realized by a Proximity Lithography Process. *Rev. Sci. Instrum.* **2006**, *77*, 043708.
(14) Pedrosa, V. A.; Miwa, D.; Machado, S. A. S.; Avaca, L. A. On the Utilization of Boron Doped Diamond Electrode as a Sensor for Parathion and as an Anode for Electrochemical Combustion of Parathion. *Electroanalysis* **2006**, *18*, 1590−1597.
(15) Regan, E. M.; Taylor, A.; Uney, J. B.; Dick, A. D.; May, P. W.; McGeehan, J. Spatially Controlling Neuronal Adhesion and Inflammatory Reactions on Implantable Diamond. *IEEE J. Emerging Sel. Topics Circuits Syst.* **2011**, *1*, 557−565.
(16) Edgington, R. J.; Thalhammer, A.; Welch, J. O.; Bongrain, A.; Bergonzo, P.; Scorsone, E.; Jackman, R. B.; Schoepfer, R. Patterned Neuronal Networks Using Nanodiamonds and the Effect of Varying Nanodiamond Properties on Neuronal Adhesion and Outgrowth. *J. Neural Eng.* **2013**, *10*, 056022.
(17) May, P. W.; Regan, E. M.; Taylor, A.; Uney, J.; Dick, A. D.; Mcgeehan, J. Spatially controlling neuronal adhesion on CVD diamond. *Diamond Relat. Mater.* **2012**, *23*, 1−5.
(18) Bonnauron, M.; Saada, S.; Rousseau, L.; Lissorgues, G.; Mer, C.; Bergonzo, P. High Aspect Ratio Diamond Microelectrode Array for Neuronal Activity Measurements. *Diamond Relat. Mater.* **2008**, *17*, 1399−1404.
(19) Bergonzo, P.; Bongrain, A.; Scorsone, E.; Bendali, A.; Rousseau, L.; Lissorgues, G.; Mailley, P.; Li, Y.; Kauffmann, T.; Goy, F.; Yvert, B.; Sahel, J. A.; Picaud, S. 3D Shaped Mechanically Flexible Diamond Microelectrode Arrays for Eye Implant Applications: The MEDINAS Project. *IRBM* **2011**, *32*, 91−94.
(20) Cottance, M.; Nazeer, S.; Rousseau, L.; Lissorgues, G.; Bongrain, A.; Kiran, R.; Scorsone, E.; Bergonzo, P.; Bendali, A.; Picaud, S.; Joucla, S.; Yvert, B. Diamond Micro-Electrode Arrays (MEAs): A New Route for in-Vitro Applications. Presented at the *2013 Symposium on Design, Test, Integration and Packaging of MEMS/MOEMS (DTIP)*, Noisy-le-Grand, France, Apr 16−18, 2013.
(21) Taniguchi, J.; Tokano, Y.; Miyamoto, I.; Komuro, M.; Hiroshima, H. Diamond Nanoimprint Lithography. *Nanotechnology* **2002**, *13*, 592−596.
(22) Ding, G.; Yao, J.; Yu, A.; Zhao, X.; Wang, L.; Shen, T. Patterning of Diamond Films by RIE and Its MEMS Aplications. In *Micromachining and Microfabrication Process Technology VI*; Karam, J. M., Yasaitis, J. A., Eds.; SPIE Press: Bellingham, WA, 2000; Vol. *4174*, pp 451−461.
(23) Ramanathan, M.; Darling, S. B.; Sumant, A. V.; Auciello, O. Nanopatterning of Ultrananocrystalline Diamond Thin Films via Block Copolymer Lithography. *J. Vac. Sci. Technol. A* **2010**, *28*, 979−983.
(24) Ando, Y.; Kuwabara, J.; Suzuki, K.; Sawabe, A. Patterned Growth of Heteroepitaxial Diamond. *Diamond Relat. Mater.* **2004**, *13*, 1975−1979.
(25) Maybeck, V.; Edgington, R.; Bongrain, A.; Welch, J. O.; Scorsone, E.; Bergonzo, P.; Jackman, R. B.; Offenhäusser, A. Boron-Doped Nanocrystalline Diamond Microelectrode Arrays Monitor Cardiac Action Potentials. *Adv. Healthcare Mater.* **2014**, *3*, 283−289.
(26) Domonkos, M.; Izak, T.; Stolcova, L.; Proska, J.; Kromka, A. Fabrication of Periodically Ordered Diamond Nanostructures by Microsphere Lithography. *Phys. Status Solidi B* **2014**, *251*, 2587−2592.
(27) Wang, X. D.; Hong, G. D.; Zhang, J.; Lin, B. L.; Gong, H. Q.; Wang, W. Y. Precise Patterning of Diamond Films for MEMS Application. *J. Mater. Process. Technol.* **2002**, *127*, 230−233.
(28) Narayan, J.; Chen, X. Laser Patterning of Diamond Films. *J. Appl. Phys.* **1992**, *71*, 3795.
(29) Ral'Chenko, V. G.; Korotushenko, K. G.; Smolin, A. A. Fine Patterning of Diamond Films by Laser-Assisted Chemical Etching in Oxygen. *Diamond Relat. Mater.* **1995**, *4*, 893−896.
(30) Shimoni, O.; Cervenka, J.; Karle, T. J.; Fox, K.; Gibson, B. C.; Tomljenovic-Hanic, S.; Greentree, A. D.; Prawer, S. Development of a Templated Approach to Fabricate Diamond Patterns on Various Substrates. *ACS Appl. Mater. Interfaces* **2014**, *6*, 8894−8902.
(31) Chen, Y.-C.; Tzeng, Y.; Cheng, A.-J.; Dean, R.; Park, M.; Wilamowski, B. M. Inkjet Printing of Nanodiamond Suspensions in Ethylene Glycol for CVD Growth of Patterned Diamond Structures and Practical Applications. *Diamond Relat. Mater.* **2009**, *18*, 146−150.
(32) Fox, N. A.; Youh, M. J.; Steeds, J. W.; Wang, W. N. Patterned Diamond Particle Films. *J. Appl. Phys.* **2000**, *87*, 8187−8191.
(33) Zhuang, H.; Song, B.; Staedler, T.; Jiang, X. Microcontact Printing of Monodiamond Nanoparticles: An Effective Route to Patterned Diamond Structure Fabrication. *J. Phys. Chem. C* **2011**, *27*, 11981−11989.
(34) Lee, S.-K.; Kim, J.-H.; Jeong, M.-G.; Song, M.-J.; Lim, D.-S. Direct Deposition of Patterned Nanocrystalline CVD Diamond Using an Electrostatic Self-Assembly Method with Nanodiamond Particles. *Nanotechnology* **2010**, *21*, 505302.
(35) Hébert, C.; Scorsone, E.; Bendali, A.; Kiran, R.; Cottance, M.; Girard, H. A.; Degardin, J.; Dubus, E.; Lissorgues, G.; Rousseau, L.; Picaud, S.; Bergonzo, P. Boron Doped Diamond Biotechnology: From Sensors to Neurointerfaces. *Faraday Discuss.* **2014**, *172*, 47−59.
(36) Cheng, N.-S. Formula for the Viscosity of a Glycerol−Water Mixture. *Ind. Eng. Chem. Res.* **2008**, *47*, 3285−3288.
(37) Kulakova, I. I. Surface Chemistry of Nanodiamonds. *Phys. Solid State* **2004**, *46*, 636−643.
(38) Ascarelli, P.; Fontana, S. Dissimilar Grit-Size Dependence of the Diamond Nucleation Density on Substrate Surface Pretreatments. *Appl. Surf. Sci.* **1993**, *64*, 307−311.
(39) Williams, O. A. Nanocrystalline Diamond. *Diamond Relat. Mater.* **2011**, *20*, 621−640.
(40) Avigal, Y.; Hoffman, A. A New Method for Nucleation Enhancement of Diamond. *Diamond Relat. Mater.* **1999**, *8*, 127−131.
(41) Osswald, S.; Mochalin, V. N.; Havel, M.; Yushin, G.; Gogotsi, Y. Phonon Confinement Effects in the Raman Spectrum of Nanodiamond. *Phys. Rev. B* **2009**, *80*, 075419.
(42) Sun, K. W.; Wang, J. Y.; Ko, T. Y. Raman Spectroscopy of Single Nanodiamond: Phonon-Confinement Effects. *Appl. Phys. Lett.* **2008**, *92*, 153115.
(43) Ferrari, A.; Robertson, J. Interpretation of Raman Spectra of Disordered and Amorphous Carbon. *Phys. Rev. B* **2000**, *61*, 14095−14107.
(44) Ondič, L.; Dohnalová, K.; Ledinský, M.; Kromka, A.; Babchenko, O.; Rezek, B. Effective Extraction of Photoluminescence from a Diamond Layer with a Photonic Crystal. *ACS Nano* **2011**, *5*, 346−350.
(45) Nebel, C. E.; Shin, D.; Rezek, B.; Tokuda, N.; Uetsuka, H.; Watanabe, H. Diamond and Biology. *J. R. Soc., Interface* **2007**, *4*, 439−461.
(46) Hees, J.; Heidrich, N.; Pletschen, W.; Sah, R. E.; Wolfer, M.; Williams, O. A.; Lebedev, V.; Nebel, C. E.; Ambacher, O. Piezoelectric Actuated Micro-Resonators Based on the Growth of Diamond on Aluminum Nitride Thin Films. *Nanotechnology* **2012**, *24*, 025601.

DOI: 10.1021/am507900a
ACS Appl. Mater. Interfaces 2015, 7, 6490−6495